Catalysis Today 175 (2011) 310–315

Contents lists available at ScienceDirect

Catalysis Today

journal homepage: www.elsevier.com/locate/cattod

Photocatalytic destruction of air pollutants with vacuum ultraviolet (VUV) irradiation

Haibao Huang*, Dennis Y.C. Leung, Guisheng Li, Michael K.H. Leung, Xianliang Fu

Department of Mechanical Engineering, The University of Hong Kong, Pokfulam Road, Hong Kong, China

ARTICLE INFO

Article history:
Received 15 September 2010
Received in revised form 29 January 2011
Accepted 6 April 2011
Available online 8 May 2011

Keywords:
Vacuum ultraviolet irradiation
Photocatalysis
Toluene
Escherichia coli
Air pollutants
Byproducts

ABSTRACT

Photocatalysis with vacuum ultraviolet (VUV) irradiation (VUV–PCO) was utilized to destroy air pollutants. *Escherichia coli* (*E. coli*) and toluene were chosen as the target pollutants. Two parallel reactions with 254 nm UV irradiation (254 nm-PCO) and without TiO_2 (i.e. VUV photolysis) were also conducted for comparison. Results indicate that VUV–PCO process has a higher efficiency in destroying toluene and inactivating *E. coli*. In addition, the stability of PCO activity is increased while the byproducts yield is lowered during toluene destruction in the VUV–PCO process. Toluene removal efficiency (TRE) in the VUV–PCO process was more than 5 times higher than that in the 254 nm-PCO process. VUV–PCO overcomes some drawbacks of conventional photocatalysis, such as low efficiency and easy photocatalyst deactivation. The destroying mechanism of air pollutants in the VUV–PCO process is greatly different from that of the 254 nm-PCO process. The excellent performance of VUV–PCO system may be attributed to the more reaction processes (such as VUV photolysis and catalytic ozonation) and more reactive species (such as active oxygen and hydroxyl radicals) formed to destroy the pollutants.

1. Introduction

Air pollution causes great harm to the environment and human health. Air pollutants, including biological and gaseous pollutants, coexist in ambient as well as in indoor environment and require simultaneous removal for better air quality [1]. Although there are lots of studies on air pollutant control, most of these studies so far only focus on the removal of a single type of air pollutants [2,3]. Presently, it is usually hard to efficiently destroy the multiple air pollutants using one single air cleaning technology.

Photocatalytic oxidation (PCO) is an innovative and promising approach to purifying indoor air [1]. It has been widely studied for the removal of gaseous [4–6] and biological pollutants [7–9]. The most widely used UV sources in PCO are 254 nm [2,5] and 365 nm UV lamp [7,9]. These PCO processes are restricted in application due to the disadvantages such as photocatalyst deactivation [10,11], electron–hole recombination [12,13] and low efficiency [14–16]. Therefore, many efforts have been made to improve PCO efficiency by combining photocatalysis with ozone [15,17,18], microwave [19,20] and magnetic field [21]. However, an extra apparatus is needed for the assisted PCO processes, causing higher operating cost and energy consumption, and more severe reaction conditions. Recently, vacuum ultraviolet (VUV) irradiated photocatalsyis (VUV–PCO) has attracted much attention in the purification of gaseous pollutants [22,23]. VUV light, generally referring to wavelengths below 200 nm, can emit energetic photons while O_3 will be produced in the presence of oxygen with VUV irradiation. Previous studies show that gaseous pollutants, such as formaldehyde and chlorinated hydrocarbons, can be directly destroyed by VUV irradiation [23,24]. Nevertheless, the VUV photolysis alone is limited in usage due to the formation of harmful byproducts such as O_3 and acetaldehyde [22,23]. Both PCO and VUV photo-degradation have their own limitations. It is therefore of much practical significance to improve the performance of PCO and VUV photolysis. The combination of VUV and PCO is a good way to improve the PCO and VUV performance. The previous study on the VUV–PCO process mainly focuses on the purification of a single gaseous pollutant [22,23], however, little attention is paid to the disinfection and intermediates, which are necessary to promote the research and application of VUV–PCO technology.

The present study aimed to obtain a stronger ability to destroy the air pollutants and overcome the limitations of the conventional PCO process using VUV–PCO. *Escherichia coli* and toluene, which are widely used bacteria and VOC in photocatalytic destruction studies, were chosen as the target pollutants. As an economical and efficient technology, VUV–PCO combines the merits of O_3, photolysis and photocatalysis in pollutant destruction. As far as we know, this is the first study on the *E. coli* inactivation and toluene destroying by the VUV–PCO process. The gaseous by-products of toluene

* Corresponding author. Tel.: +852 22194547; fax: +852 28585415.
E-mail addresses: seabao8@gmail.com, harbor@hku.hk (H. Huang).

0920-5861/$ – see front matter © 2011 Elsevier B.V. All rights reserved.
doi:10.1016/j.cattod.2011.04.015

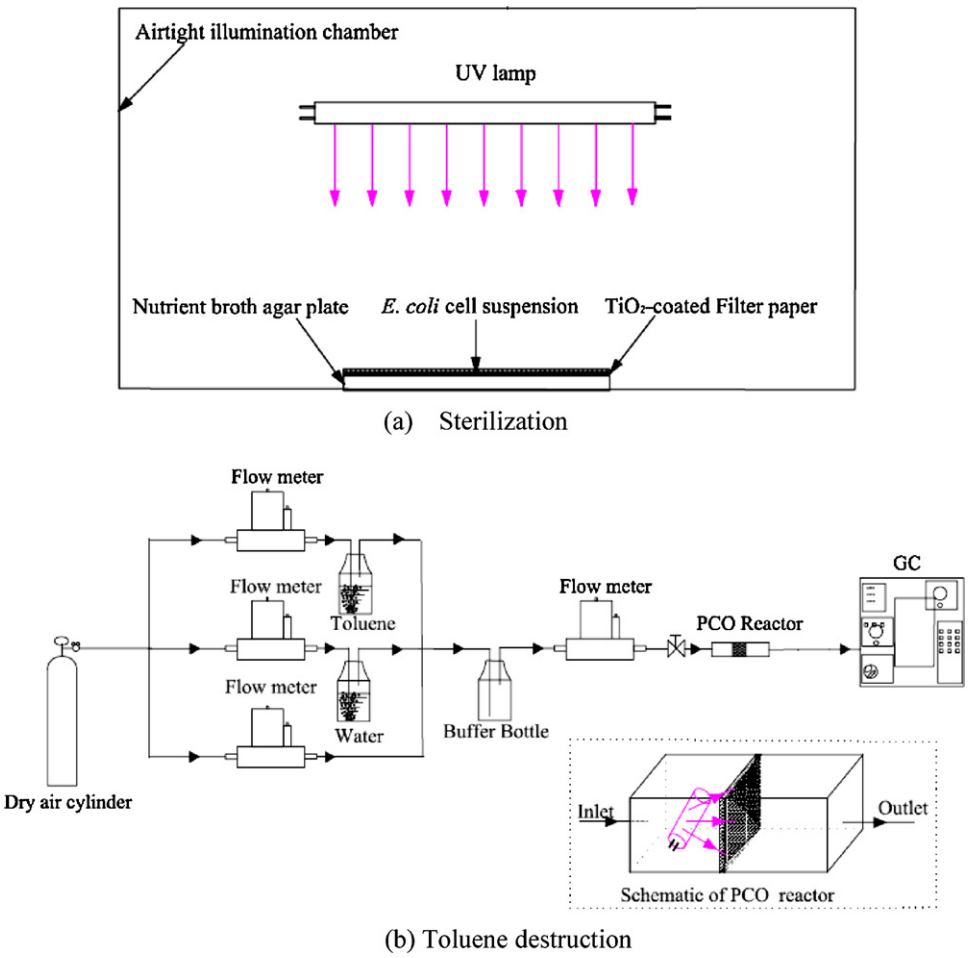

Fig. 1. Experimental setup: (a) sterilization; (b) toluene destruction.

oxidation were identified by GC–MS. Generally, the present work provides a novel way to efficiently destroy multiple air pollutants and improve the PCO performance. It also allows a new insight into the air pollutants destroying mechanism in the VUV–PCO process and makes a valuable basis for its application.

2. Experimental

2.1. Catalyst preparation

Nano-TiO_2 (P-25, Degussa) was dispersedly loaded on a γ-Al_2O_3/nickel foam support in the form of mesh by impregnation method. Briefly, the porous nickel foam support, with the size of 10 cm × 10 cm × 0.2 cm (length × width × thickness), was impregnated in the sol solution of $Al_2O_3{\cdot}nH_2O$, then dried at 373 K for 2 h and calcined at 850 K for 4 h to get the γ-Al_2O_3/nickel foam support. TiO_2 was put into distilled water and dispersed fully in an ultrasonic cleaner bath to get 8 wt% TiO_2 slurry. The γ-Al_2O_3/nickel foam support was dipped into the TiO_2 slurry, impregnated for 30 min and then dried at 100 for 2 h. The loaded TiO_2 on the support is 1.0 g.

The TiO_2/γ-Al_2O_3/nickel foam photocatalyst has a pentagonal framework and low pressure drop. Such 3D structure can improve the molecular transport of reactants and products. It also allows light to penetrate easily into the inner body of the catalyst to enhance the utilization efficiency of light in the photocatalytic reaction.

2.2. Experimental setup

2.2.1. Experiment I: sterilization experiments

The experimental setup for sterilization was shown in Fig. 1a. *E. coli* (strain M15) was used as a model bacterium in this evaluation. All materials used in the experiments were autoclaved at 394 K for 30 min to ensure sterility. *E. coli* was inoculated into Luria–Bertani (LB) nutrient broth (10 g/L tryptone, 5 g/L yeast extract, and 5 g/L NaCl) at 310 K for 2 h. The treated cells were then resuspended and diluted. 10 μL of *E. coli* cell suspension was pipetted onto each TiO_2-coated and uncoated filter paper (2 cm × 2 cm). The filter paper samples supported *E. coli* were separately illuminated with 254 nm UV lamp (4 W, Philips) and VUV lamp (4 W, Cnlight) in an airtight illumination chamber for 5 min, respectively (see Fig. 1a). The VUV lamp has a peak spectral emissive power at 254 nm and a smaller (about 8%) emission at 185 nm. After illumination, the cell suspension was collected by washing the filter paper with 5 ml 0.9% saline solution. Then the collected cells suspension was diluted appropriately, and 0.5 ml diluted suspension was spread on the nutrient broth agar plate and incubated at 310 K for 24 h. Two parallel experiments were conducted for comparison under the same conditions. One is a blank experiment, in which there is no *E. coli* inoculated and UV irradiation. The other is a dark control experiment, in which there is *E. coli* inoculated but without any UV irradiation.

2.2.2. Experiment II: toluene destruction

The experimental setup and the PCO reactor for toluene destruction were shown in Fig. 1b. A continuous-flow honey-

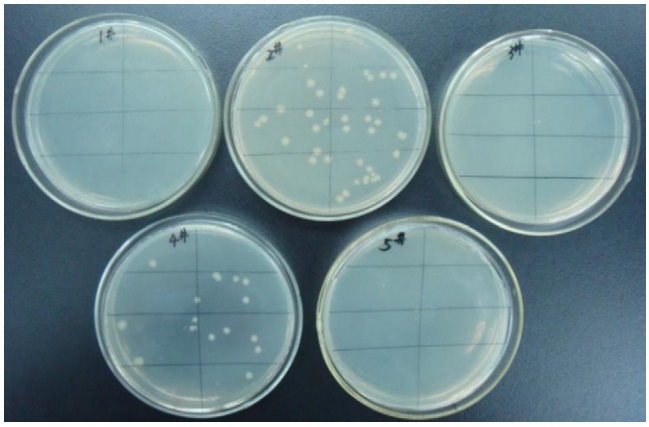

Fig. 2. Microbial colonies obtained in the culture plates after incubation for 24 h under different conditions 1#: blank; 2#: without UV irradiation (dark control tests); 3#: VUV–PCO for 5 min; 4#: VUV irradiation for 5 min; 5#: 254 nm-PCO for 5 min.

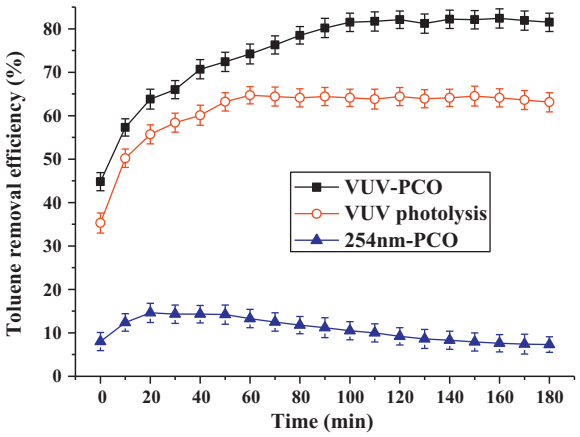

Fig. 3. Toluene removal efficiency in different processes.

comb type reactor was used in the experiment. The PCO reactor is a rectangle container with sizes of 30 cm × 15 cm × 10 cm (length × width × height). The photocatalyst mesh was fixed in the centre of the reactor, as shown in Fig. 1a. UV irradiation was provided by a 254 nm UV lamp and VUV lamp, separately. The air flow rate, initial toluene and water vapor content at the inlet of the PCO reactor were 1 L/min, 50 ppm and 1 wt%, respectively.

Toluene in the air stream was analyzed on-line by a gas chromatograph (GC-2010, Shimadzu) equipped with a FID. The gaseous organic intermediates were concentrated from the outlet gas by an adsorption bottle filled with methanol. The absorption solution was then analyzed by GC–MS (QP2010, Shimadzu).

3. Results and discussion

3.1. Inactivation of E. coli

Fig. 2 shows the microbial colonies obtained in the culture plates under different conditions. No trace of *E. coli* was found in the blank experiment (1#) while 39 colonies of *E. coli* survived in the dark control experiment (2#). In the VUV irradiation experiment (4#), 15 colonies of *E. coli* survived. Only about 62% *E. coli* was killed after VUV irradiation. Irradiation of UV (185 nm and 254 nm) can cause direct DNA damage by inducing the formation of DNA photoproducts. The accumulation of DNA photoproducts can be lethal to cells through the blockage of DNA replication and RNA transcription [25].

As shown in Fig. 2, no *E. coli* survived for both VUV–PCO (3#) and 254 nm-PCO processes (5#). The bacterial inactivation is strongly enhanced in the presence of TiO_2. When TiO_2 is irradiated by UV light, excited pairs of electrons and holes are generated. The photogenerated holes react with the water to produce highly reactive hydroxyl radicals (•OH) that can kill bacteria. Oxidative attack of the cell membrane led to the lipid peroxidation. The combination of cell membrane damage, and further oxidative attack of internal cellular components, ultimately resulted in cell death [25–27].

There are more processes to inactivate *E. coli* in the VUV–PCO process besides PCO and UV irradiation. Much O_3 (30 ppm) can be generated from VUV lamp. O_3 and the reactive oxidants such as •OH and atomic oxygen formed from O_3 catalytic decomposition can also kill *E. coli* efficiently. Thus, VUV–PCO has better disinfection efficiency than individual UV irradiation, O_3 or 254 nm-PCO.

In the present study, the difference in antibacterial effect between the VUV–PCO and 254 nm-PCO process is not significant due to the fact that •OH formed in both process was sufficient for sterilizing the experimental *E. coli*.

The most common air disinfection method is UV irradiation. However, it could only disinfect airborne bacteria close to the lamps as UV light has limited penetration capacity. In case of a contaminated room, UV disinfection alone is inadequate to provide virus-free environment. O_3 is a powerful oxidizer and can kill microorganisms effectively with good penetration capability and flowability. In contrast to UV irradiation, O_3 could penetrate to every corners of environment, thus it could effectively disinfect airborne bacteria. However, its application in air disinfection is limited due to the concern on ozone's toxicity. O_3 has adverse effects on human health and its use for air disinfection is generally not recommended in the presence of occupants in the room. Sterilization by VUV–PCO has the advantages of disinfection with individual UV irradiation and O_3, and overcoming their drawbacks. Residual O_3 can be removed by catalytic decomposition and further enhance air disinfection in the VUV–PCO process.

3.2. Destruction of toluene

Toluene destruction effects by VUV–PCO, VUV photolysis and 254 nm-PCO processes were compared. As shown in Fig. 3, maximum toluene removal efficiency (TRE) was only 14.3% in the 254 nm-PCO process, whereas, the stable TRE reached 63.9% in the VUV photolysis process. VUV–PCO yielded the highest TRE, reaching about 82.1%. The TRE was notably increased in the VUV–PCO process, compared with that in the 254 nm-PCO and VUV photolysis process.

PCO reaction is typically governed by the generation of •OH which is generally regarded as a primary strong oxidant in the 254 nm-PCO process [15,17,18]. In the 254 nm-PCO process, •OH was mainly formed via Eqs. (1)–(3) [15,17,18]:

$$TiO_2 + h\nu \rightarrow TiO_2 + e^- + h^+ \quad (1)$$

$$h^+ + H_2O \rightarrow {}^\bullet OH + H^+ \quad (2)$$

$$h^+ + OH^- \rightarrow {}^\bullet OH \quad (3)$$

The •OH formed is inadequate for toluene oxidation due to the electron–hole recombination, resulting in the low TRE in the 254 nm-PCO process as observed. Compared with 254 nm-PCO, VUV photolysis obtained much higher TRE. 254 nm-PCO is generally considered as heterogeneous catalysis in which toluene oxidation mainly occurs on the surface of photocatalyst. However, toluene destruction by VUV photolysis occurs in the gas phase, which is greatly different from that in 254 nm-PCO. More reactive oxidants are formed for toluene destruction in the VUV photolysis process.

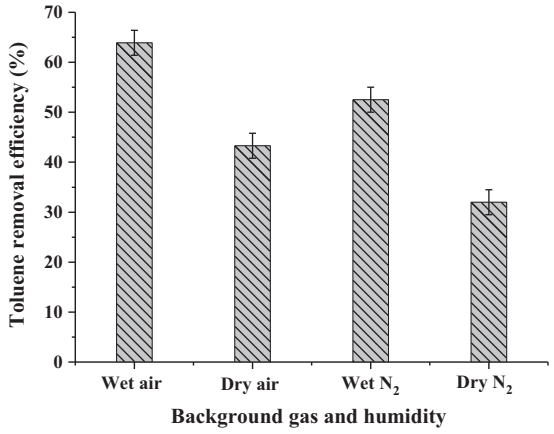

Fig. 4. Effect of reaction medium and water vapor on the toluene removal efficiency in the VUV photolysis process.

Oxygen in air is dissociated and accordingly O_3 is formed under VUV irradiation via Eqs. (4)–(6) [16,23,28].

$$O_2 + h\nu(< 243\,\text{nm}) \rightarrow O(^1D) + O(^3P) \quad (4)$$

$$O(^1D) + M \rightarrow O(^3P) + M \quad (M = O_2 \text{ or } N_2) \quad (5)$$

$$O(^3P) + O_2 + M \rightarrow O_3 + M \quad (6)$$

where $O(^1D)$ and $O(^3P)$ represent excited and ground state oxygen atom, respectively. Toluene can be oxidized by the atomic oxygen, which is the intermediate during the O_3 formation. $O(^1D)$ is also formed from O_3 decomposition by UV irradiation via Eq. (7) [28],

$$O_3 + h\nu(< 310\,\text{nm}) \rightarrow O(^1D) + O_2 \quad (7)$$

Besides $O(^1D)$, the •OH can also be abundantly produced via Eqs. (8) and (9) in the presence of water vapor in the VUV process [16,23]:

$$O(^1D) + H_2O \rightarrow {}^\bullet OH \quad (8)$$

$$H_2O + h\nu(185\,\text{nm}) \rightarrow {}^\bullet OH + H \quad (9)$$

The •OH and atomic oxygen formed can efficiently oxidize toluene presented in the air stream. In addition, toluene can also be directly destroyed through VUV photolysis. UV light with 185 nm wavelength corresponds to a photon energy of 6.7 eV which is larger than the energies of the C–H bond in the methyl (3.7 eV) and aromatic ring (4.3 eV), of the C–C bond in the methyl (4.4 eV), of the C–C bond in the aromatic ring (5.0–5.3 eV) and of the C=C bond in the aromatic ring (5.5 eV) of toluene [29]. Energetic photons can efficiently break down the chemical bonds of toluene and destroy toluene.

In order to make out toluene destruction by the energetic photons, atomic oxygen and •OH in the VUV process, experiments were carried out under different conditions. Fig. 4 shows the effect of reaction medium and water vapor on the TRE. It is only 32% in the dry N_2 stream. Since nitrogen does not absorb light above 125 nm, and no oxidative reaction occurs under that condition, toluene destruction in a dry nitrogen stream should be due to photodegradation of energetic photons only [28]. The TRE is increased to 52.5% in the wet N_2 stream with 1% humidity, in which both photolysis and the •OH contributes to the toluene destruction. The •OH can be formed from water dissociation with the 185 nm UV irradiation, as described in Eq. (9). The •OH formed can enhance toluene oxidation. The TRE is 43.3% in the dry air stream, in which toluene destruction is due to both energetic photons and atomic oxygen. However, it is increased to 63.9% in the wet air stream with 1% humidity, in which the •OH is also responsible for toluene destruction besides energetic photons and atomic oxygen. The TRE is increased remarkably in both N_2 and air stream with water vapor, compared with the dry stream. Since water molecules exhibit a continuous UV adsorption spectrum between 175 and 190 nm, much •OH can be produced in the gas phase [30]. The TRE in the dry air stream (43.3%) is higher compared with that in the dry N_2 stream (32%). The TRE in the wet air stream (63.9%) is higher than that in the wet N_2 stream (52.5%). Compared with N_2 stream, it is increased in both dry and wet stream in the presence of oxygen. The formed atomic oxygen and •OH enhanced TRE in the air stream. Therefore, both energetic photons and highly reactive radicals (i.e. atomic oxygen and •OH) are responsible for the toluene destruction in the VUV photolysis process.

Toluene destruction in the VUV–PCO process is greatly different from that in the 254 nm-PCO process. In the 254 nm-PCO process, toluene destruction was mainly attributed to the •OH formed on the catalyst while the 254 nm UV light itself hardly contribute to toluene degradation. However, more processes (such as VUV photolysis, catalytic ozonation) are involved in the toluene destruction in the VUV–PCO process. It combines the merits of O_3, VUV photolysis and 254 nm-PCO process. TiO_2 can be irradiated by the 185 nm and 254 nm UV light, leading to photocatalytic oxidation. In addition, O_3 generated from the VUV lamp can greatly enhance toluene destruction with higher removal efficiency and better PCO durability [17,18,31]. In the meanwhile, O_3, with higher electron affinity than oxygen, can reduce the recombination rate of photogenerated electron–hole pairs and increase the formation rate of •OH [32–34]. What is more, O_3 can be catalytically decomposed by TiO_2, forming more •OH and atomic oxygen via Eqs. (10) and (11):

$$O_3 + * \rightarrow O* + O_2 \quad (10)$$

$$O + H_2O \rightarrow 2OH^\bullet \quad (11)$$

where * denotes an active site on the surface of photocatalyst.

Photochemical oxidation occurs in the gas-phase while PCO oxidation and catalytic ozonation occur over the TiO_2 catalyst. The increased TRE in the VUV–PCO process is mainly attributed to increased pathways to form highly reactive species for toluene destruction. Toluene destruction happened both in the gas-phase and on the surface of photocatalyst. Accordingly, toluene could be destroyed more quickly by VUV–PCO than the other two processes. Among the multiple processes in the VUV–PCO system, VUV photolysis played a key role in toluene destruction. As shown in Fig. 3, the TRE reached 63.9% in the VUV photolysis process.

It can be observed that the TRE in the PCO process gradually dropped after operation for 50 min (Fig. 3), indicating that the photocatalyst was easily deactivated. However, this phenomenon was not observed in the VUV–PCO process even after operation for 3 h. The TRE in the VUV–PCO process kept stable after operation for about 100 min (Fig. 3). The enhanced durability of PCO activity in the VUV–PCO process is probably due to the following facts: (i) more reactive oxidants were formed, resulting in complete oxidation of toluene and less byproducts formed on the surface of the photocatalysts; and (ii) some toluene was destroyed by VUV photolysis in the gas-phase before the PCO reaction.

3.3. By-products of toluene destruction

The possible byproducts of the toluene destruction process include residual O_3 and organic intermediates.

3.3.1. Residual ozone

The biggest problem with VUV photolysis is the possible pollution caused by residual O_3. The formation of O_3 with the VUV irradiation is described in Eqs. (4)–(6). As shown in Fig. 5, no O_3 was detected in the air stream of the 254 nm-PCO process while the O_3 concentration reached 30 ppm in the effluent of the VUV pho-

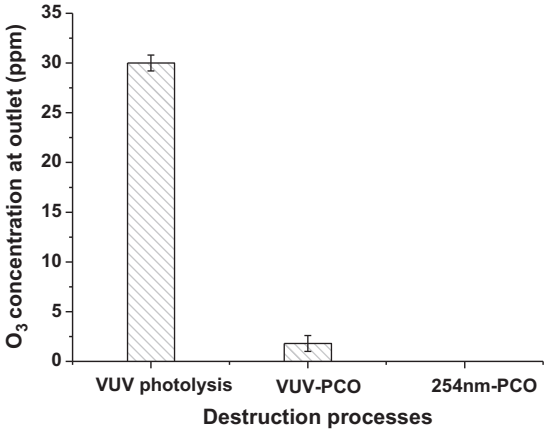

Fig. 5. O_3 concentrations in the effluent in different processes.

tolysis reactor. It dramatically dropped from 30 ppm to 1.8 ppm in the VUV–PCO process compared to the VUV process. The O_3 level was greatly reduced with the photocatalyst. As such, the O_3 concentration in the effluent of VUV–PCO process can be easily reduced to a safer level by increasing the catalyst loading or improving the catalytic performance for O_3 decomposition. O_3 level is reduced mainly through two pathways in this process: decomposition by photolysis and catalysts, consumption by acting as electron acceptor and scavenger to •OH [15,18]. Among them, catalytic destruction played an important role in the O_3 destruction. As shown in Eqs. (7), (8), (10) and (11), highly reactive •OH and atomic oxygen were produced during the O_3 decomposition, which can further enhance toluene oxidation. Therefore, the residual O_3 and unreacted toluene can be simultaneously eliminated in the VUV–PCO process. In a previous study, an O_3 decomposition catalyst (ODC) layer was set up behind the photoreactor in order to eliminate excess O_3 in the effluent gas stream [28]. However, additional ODC layer will complicate the setup and add extra cost. In this experiment, most of the residual O_3 can be eliminated without the need of an additional ODC layer.

3.3.2. Organic by-products

Toxic by-products from incomplete oxidation of VOCs are also a serious challenge for practical application of photolysis [28,35]. The gaseous byproducts formed in the VUV photolysis process are mainly formic acid, acetic acid, benzaldehyde and benzoic acid (Fig. 6a). In the VUV photolysis process, decomposition of toluene mainly occurs in the gas-phase, and intermediates of toluene oxidation are directly discharged with the effluent gas stream. However, the byproducts are greatly reduced in the VUV–PCO process, compared with the VUV photolysis process. Only formic acid, acetic acid and benzaldehyde were identified by GC–MS (Fig. 6b) while the benzoic acid and benzyl alcohol was not found in the VUV–PCO process. The gaseous intermediates from toluene photo-degradation could be trapped by the catalyst mesh and further oxidized by the •OH and atomic oxygen generated, leading to the reduction of by-products in the VUV–PCO process.

During toluene oxidation in the 254 nm-PCO process, less-reactive intermediates are responsible for the deactivation of catalyst. These intermediates are strongly adsorbed onto the surface of the TiO_2 catalyst and deteriorate its photocatalytic activity by blocking its reaction sites [10,11,15]. Benzaldehyde, formic acid and acetic acid were identified by GC–MS in the 254 nm-PCO process, which was consistent with the results of the previous study [5,36,37]. The intermediates generated from toluene oxidation resulted in the quick deactivation of photocatalysts in the PCO process. The intensity of formic acid and acetic acid is a little higher

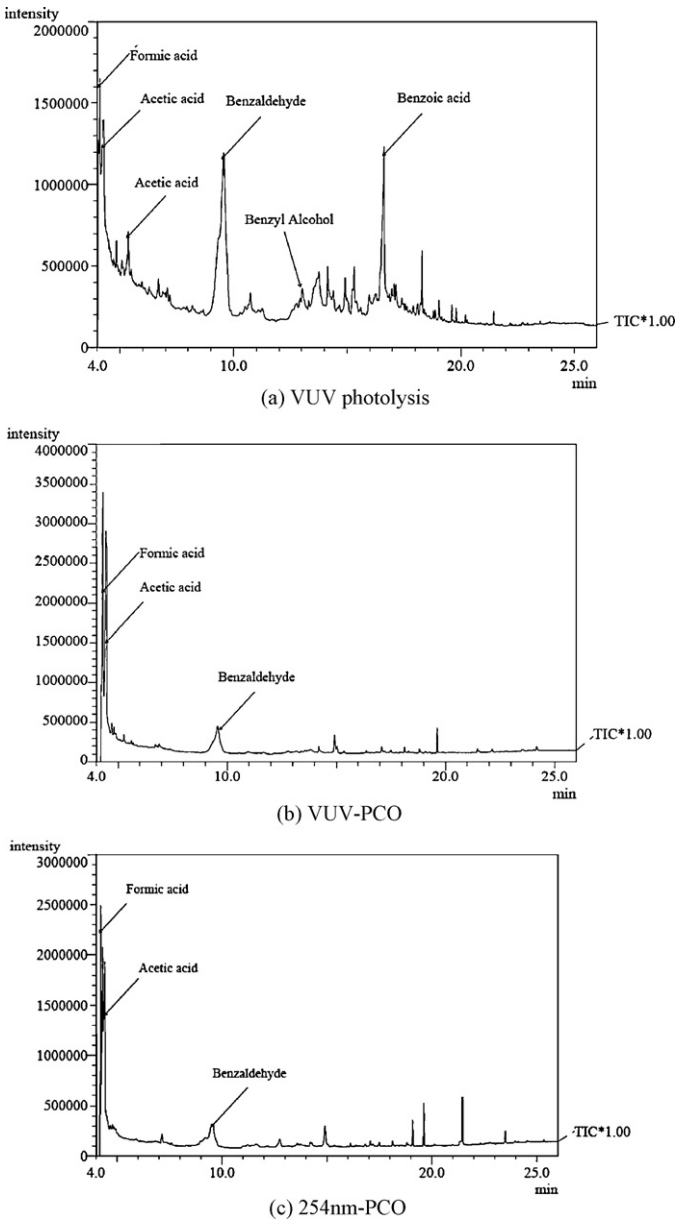

Fig. 6. GC–MS chromatogram of the gaseous byproducts of toluene decomposition by (a) VUV photolysis; (b) VUV–PCO; (c) 254 nm-PCO.

than that of 254 nm-PCO and VUV photolysis due to the fact that the amount of toluene oxidized in the VUV–PCO process was larger than the other two processes.

4. Conclusions

VUV–PCO process has a higher efficiency in destroying toluene and inactivating *E. coli*, compared with the 254 nm-PCO and VUV photolysis processes. In addition, the stability of PCO activity is increased while the yield of byproducts such as O_3 and organic compounds is reduced during toluene destruction in the VUV–PCO process. The TRE in the VUV–PCO process was more than 5 times higher than that of 254 nm-PCO. VUV–PCO can overcome some drawbacks of conventional photocatalysis, such as low efficiency and easy photocatalyst deactivation. The destroying mechanism of air pollutants in the VUV–PCO process is greatly different from that of the 254 nm-PCO process. The excellent performance of VUV–PCO system may be attributed to the more reaction processes (such as

VUV photolysis and catalytic ozonation) and more reactive species formed to destroy the pollutants.

Acknowledgments

The authors gratefully acknowledge the financial supports from the CRCG of the University of Hong Kong (Grant No. 200907176159).

References

[1] B.F. Yu, Z.B. Hu, M. Liu, H.L. Yang, Q.X. Kong, Y.H. Liu, Review of research on air-conditioning systems and indoor air quality control for human health, Int. J. Refrig. 32 (2009) 3–20.
[2] F.N. Chen, X.D. Yang, Q. Wu, Photocatalytic oxidation of Escherichia coli, Aspergillus niger, and formaldehyde under different ultraviolet irradiation conditions, Environ. Sci. Technol. 43 (2009) 4606–4611.
[3] W. Chen, J.S. Zhang, UV-PCO device for indoor VOCs removal: investigation on multiple compounds effect, Build. Environ. 43 (2008) 246–252.
[4] L.X. Cao, Z. Gao, S.L. Suib, Photocatalytic oxidation of toluene on nanoscale TiO_2 catalysts: studies of deactivation and regeneration, J. Am. Chem. Soc. 220 (2000) 269–1269.
[5] J. Mo, Y. Zhang, Q. Xu, Y. Zhu, J.J. Lamson, R. Zhao, Determination and risk assessment of by-products resulting from photocatalytic oxidation of toluene, Appl. Catal. B: Environ. 89 (2009) 570–576.
[6] M. Sleiman, P. Conchon, C. Ferronato, J.-M. Chovelon, Photocatalytic oxidation of toluene at indoor air levels (ppbv): towards a better assessment of conversion, reaction intermediates and mineralization, Appl. Catal. B: Environ. 86 (2009) 159–165.
[7] F. Chen, X. Yang, F. Xu, Q. Wu, Y. Zhang, Correlation of photocatalytic bactericidal effect and organic matter degradation of TiO_2. Part I. Observation of phenomena, Environ. Sci. Technol. 43 (2009) 1180–1184.
[8] A. Vohra, D.Y. Goswami, D.A. Deshpande, S.S. Block, Enhanced photocatalytic disinfection of indoor air, Appl. Catal. B: Environ. 64 (2006) 57–65.
[9] H.M. Coleman, C.P. Marquis, J.A. Scott, S.S. Chin, R. Amal, Bactericidal effects of titanium dioxide-based photocatalysts, Chem. Eng. J. 113 (2005) 55–63.
[10] E. Piera, J.A. Ayllon, X. Domenech, J. Peral, TiO_2 deactivation during gas-phase photocatalytic oxidation of ethanol, Catal. Today 76 (2002) 259–270.
[11] C. Belver, M.J. Lopez-Munoz, J.M. Coronado, J. Soria, Palladium enhanced resistance to deactivation of titanium dioxide during the photocatalytic oxidation of toluene vapors, Appl. Catal. B: Environ. 46 (2003) 497–509.
[12] L. Rideh, A. Wehrer, D. Ronze, A. Zoulalian, Photocatalytic degradation of 2-chlorophenol in TiO_2 aqueous suspension: modeling of reaction rate, Ind. Eng. Chem. Res. 36 (1997) 4712–4718.
[13] S. Peng, Y. Li, F. Jiang, G. Lu, S. Li, Effect of Be^{2+} doping TiO_2 on its photocatalytic activity, Chem. Phys. Lett. 398 (2004) 235–239.
[14] C.H. Ao, S.C. Lee, J.Z. Yu, J.H. Xu, Photodegradation of formaldehyde by photocatalyst TiO_2: effects on the presences of NO, SO_2 and VOCs, Appl. Catal. B: Environ. 54 (2004) 41–50.
[15] X. Huang, J. Yuan, J. Shi, W. Shangguan, Ozone-assisted photocatalytic oxidation of gaseous acetaldehyde on TiO_2/H-ZSM-5 catalysts, J. Hazard. Mater. 171 (2009) 827–832.
[16] P.Y. Zhang, J. Liu, Z.L. Zhang, VUV photocatalytic degradation of toluene in the gas phase, Chem. Lett. 33 (2004) 1242–1243.
[17] K.P. Yu, G.W.M. Lee, Decomposition of gas-phase toluene by the combination of ozone and photocatalytic oxidation process (TiO_2/UV. TiO_2/UV/O_3, and UV/O_3), Appl. Catal. B: Environ. 75 (2007) 29–38.
[18] P.Y. Zhang, F.Y. Liang, G. Yu, Q. Chen, W.P. Zhu, A comparative study on decomposition of gaseous toluene by O_3/UV. TiO_2/UV and O_3/TiO_2/UV, J. Photochem. Photobiol. A: Chem. 156 (2003) 189–194.
[19] C. Jou, C. Lee, C. Tsai, H. Wang, Microwave-assisted photocatalytic degradation of trichloroethylene using titanium dioxide, Environ. Eng. Sci. 25 (2008) 975–980.
[20] Z. Ai, P. Yang, X. Lu, Degradation of 4-chlorophenol by a microwave assisted photocatalysis method, J. Hazard. Mater. 124 (2005) 147–152.
[21] M. Wakasa, N. Ishii, M. Okano, Magnetic field effect on photocatalytic decomposition reaction of tert-butanol with platinized TiO_2 particles, C. R. Chimie 9 (2006) 836–840.
[22] J. Jeong, K. Sekiguchi, W. Lee, K. Sakamoto, Photodegradation of gaseous volatile organic compounds (VOCs) using TiO_2 photoirradiated by an ozone-producing UV lamp: decomposition characteristics, identification of by-products and water-soluble organic intermediates, J. Photochem. Photobiol. A: Chem. 169 (2005) 279–287.
[23] L. Yang, Z. Liu, J. Shi, Y. Zhang, H. Hu, W. Shangguan, Degradation of indoor gaseous formaldehyde by hybrid VUV and TiO_2/UV processes, Sep. Purif. Technol. 54 (2007) 204–211.
[24] T. Alapi, A. Dombi, Direct VUV photolysis of chlorinated methanes and their mixtures in an oxygen stream using an ozone producing low-pressure mercury vapour lamp, Chemosphere 67 (2007) 693–701.
[25] A.G. Rincon, C. Pulgarin, Fe^{3+} and TiO_2 solar-light-assisted inactivation of *E. coli* at field scale—implications in solar disinfection at low temperature of large quantities of water, Catal. Today 122 (2007) 128–136.
[26] Z. Huang, P.-C. Maness, D.M. Blake, E.J. Wolfrum, S.L. Smolinski, W.A. Jacoby, Bactericidal mode of titanium dioxide photocatalysis, J. Photochem. Photobiol. A: Chem. 130 (2000) 163–170.
[27] D.M. Blake, P.C. Maness, Z. Huang, E.J. Wolfrum, J. Huang, W.A. Jacoby, Application of the photocatalytic chemistry of titanium dioxide to disinfection and the killing of cancer cells, Sep. Purif. Method 28 (1999) 1–50.
[28] J. Jeong, K. Sekiguchi, K. Sakamoto, Photochemical and photocatalytic degradation of gaseous toluene using short-wavelength UV irradiation with TiO_2 catalyst: comparison of three UV sources, Chemosphere 57 (2004) 663–671.
[29] A. Ogata, D. Ito, K. Mizuno, S. Kushiyama, A. Gal, T. Yamamoto, Effect of coexisting components on aromatic decomposition in a packed-bed plasma reactor, Appl. Catal. A: Gen. 236 (2002) 9–15.
[30] C. Feiyan, S.O. Pehkonen, M.B. Ray, Kinetics and mechanisms of UV-photodegradation of chlorinated organics in the gas phase, Water Res. 36 (2002) 4203–4214.
[31] H. Qi, D.Z. Sun, G.Q. Chi, Formaldehyde degradation by UV/TiO_2/O_3 process using continuous flow mode, J. Environ. Sci. China 19 (2007) 1136–1140.
[32] B. Kasprzyk-Hordern, M. Ziek, J. Nawrocki, Catalytic ozonation and methods of enhancing molecular ozone reactions in water treatment, Appl. Catal. B: Environ. 46 (2003) 639–669.
[33] M.M. Ye, Z.L. Chen, X.W. Liu, Y. Ben, J.M. Shen, Ozone enhanced activity of aqueous titanium dioxide suspensions for photodegradation of 4-chloronitrobenzene, J. Hazard. Mater. 167 (2009) 1021–1027.
[34] V. Augugliaro, M. Litter, L. Palmisano, J. Soria, The combination of heterogeneous photocatalysis with chemical and physical operations: a tool for improving the photoprocess performance, J. Photochem. Photobiol. C: Photochem. Rev. 7 (2006) 127–144.
[35] M. Mohseni, Gas phase trichloroethylene (TCE) photooxidation and byproduct formation: photolysis vs. titania/silica based photocatalysis, Chemosphere 59 (2005) 335–342.
[36] O. d'Hennezel, P. Pichat, D.F. Ollis, Benzene and toluene gas-phase photocatalytic degradation over H_2O and HCl pretreated TiO_2: by-products and mechanisms, J. Photochem. Photobiol. A: Chem. 118 (1998) 197–204.
[37] Y. Irokawa, T. Morikawa, K. Aoki, S. Kosaka, T. Ohwaki, Y. Taga, Photodegradation of toluene over TiO_2-*x*Nx under visible light irradiation, Phys. Chem. Chem. Phys. 8 (2006) 1116–1121.